ORIGINAL PAPER

Electrochemical degradation of Reactive Red 120 using DSA and BDD anodes

T. Panakoulias · P. Kalatzis · D. Kalderis · A. Katsaounis

Abstract Electrochemical oxidation of an azo dye (Reactive Red 120) was studied in acidic media (1 M $HClO_4$) using DSA type (Ti/IrO_2–RuO_2) and boron doped diamond (BDD) anodes. Ti/IrO_2–RuO_2 exhibited low oxidation power with high selectivity to organic intermediates and low TOC removal (10% at 25 °C and 40% at 80 °C). On the other hand BDD was found to be suitable for total mineralization of the organic loading to CO_2. In both cases, the decoloration of the solution was almost 100% achieved very quickly with BDD (2 Ah L^{-1}) but only after long treatment with Ti/IrO_2–RuO_2 (25 Ah L^{-1}). The instantaneous current efficiency (ICE) was up to 0.13 in the case of Ti/IrO_2–RuO_2 and up to 0.45 in the case of BDD.

Keywords Azo dye · DSA · BDD · Electrochemical oxidation · Reactive Red 120 · Ti/IrO_2–RuO_2

1 Introduction

The development and expansion of various industries (textile, leather, paper production, food technology, agricultural, photoelectrochemical cells, hair coloring etc.) that use synthetic organic dyes is remarkable during the last decades. The quantities of wastewaters produced from these activities are continuously increasing. Regardless of the dye concentration, these wastewaters are often highly colored and turbid. In addition, many dyes and their breakdown products are toxic and/or mutagenic to life. Due to their highly polluting nature, the treatment of such wastewaters has been in the center of attention for several years.

In general, dyes are classified according to their chemical structure and application [1]. Specific groups (called chromophores) are responsible for the color of the dye, while electron withdrawing or donating substituents (called auxochromes) increase the coloring effect of the chromophores [2]. Important chromophores include the azo (–N=N–), carbonyl (–C=O), methane (–CH=), nitro (–NO$_2$) and quinoid groups. Typical auxochromes include amine (–NH$_2$), carboxyl (–COOH), sulfonate (–SO$_3$H) and hydroxyl (-OH) groups. Approximately, one million tones of dyes are produced every year all around the world. The majority (about 70% by weight) is azo dyes while anthraquinone dyes constitute the second most important class of textile dyes [3, 4].

Although biological degradation methods are one of the most economic processes for wastewater treatment, they are often ineffective to degrade molecules of refractive nature, like those present in textile industry wastewaters. Also, the survival of anaerobic biomass in the presence of high concentration of azo dyes is a difficult task. Therefore, for the treatment of this type of wastewaters other alternative methods have been proposed in the literature. The majority of them concerns advanced oxidation processes [5–25], like electrooxidation, Fenton, photocatalysis or even combination of techniques (electro-fenton, photo-electrocatalysis). In addition, technologies based on biological (aerobic and anaerobic decomposition), physico-chemical (coagulation,

T. Panakoulias · P. Kalatzis · A. Katsaounis (✉)
Department of Environmental Engineering, Technical University of Crete, Polytechneioupolis, 73100 Chania, Greece
e-mail: alex.katsaounis@enveng.tuc.gr

D. Kalderis
Department of Natural Resources and the Environment, Technological and Educational Institute of Crete, 73100 Chania, Greece

filtration, adsorption, ion exchange) and chemical methods (ozonation, with hydrogen peroxide, permanganate) have also been applied.

Several types of anodes for the electrochemical oxidation of dyes have been recently reviewed by Martínez-Huitle and Brillas [26]. Typical examples of widely used anodes include Fe [27], steel [28, 29], Al [30], Dimensionally Stable Anodes (DSA) composed of mixtures of Ti, Ir, Ru, Sn, Pb and/or Sb oxides [31–33], Pt [29, 34] or Ti-supported Pt [35], granular activated carbon [14], activated carbon fiber (ACF) [15], glassy carbon [16], graphite [17], polypyrrole [18], perovskite-like $BaPb_{0.9}Sb_{0.1}O_3$ [19] and BDD deposited mainly on Si [20], Ti [21] or Nb [7] substrates. These electrodes could be used either for direct (occurring at the surface of the anode) or for indirect oxidation processes such as the homogeneous reaction of organic pollutants with strong oxidants (like active chlorine [36], or hydroxyl radicals via Fenton's reaction [37]).

According to a modern approach in electrochemical mineralization of organic pollutants [38] different anode materials can be classified according to their oxidation power in acidic media. In general, during the electrolytic process the reaction of organics with electrogenerated hydroxyl radicals competes with the side reaction of the anodic discharge of these radicals to oxygen. Kapałka et al. [38] proposed that the weaker the interaction between the hydroxyl radicals and the electrode surface, the lower the electrochemical activity toward oxygen evolution (high overvoltage anodes) and the higher the chemical reactivity toward organics oxidation. According to this, IrO_2 and RuO_2 are considered as anodes with low oxidation power while BDD as an anode with high oxidation power. In general, electrolysis on anodes with low oxidation power results in partial oxidation products and therefore these electrodes are suitable for organic electrosynthesis. In this study, a combination of two typical anodes of low oxidation power (IrO_2 and RuO_2) has been used to explore the behavior of Ti/IrO_2–RuO_2 for the electrochemical oxidation of an azo dye (Reactive Red 120, RR120).

BDD is a relatively new electrode material which has attracted great attention due to its inert surface with weak adsorption properties, its remarkable corrosion stability even in acidic media and its high oxygen evolution overpotential [39–41]. The majority of the studies [20, 21, 39–41] have shown that BDD provides total mineralization of the organic loading with high current efficiencies.

Reactive Red 120 is widely used in color industry while there are only few reports [22–25] on its abatement with advanced oxidation processes and specifically with direct electrochemical oxidation. Zhang et al. [22] reported possible decomposition pathways and reaction intermediates formation of purified, hydrolyzed Reactive Red 120, during

ozonation. RR120 was decomposed under direct nucleophilic attack by ozone, resulting in oxidation and cleavage of the azo group and the aromatic ring, while the triazine group still remained in solution even after prolonged oxidation time (120 min) due to its resistance to ozonation. The effects of RR120 additives on the ozonation process and oxidation by-products have been studied [23] and the results showed that the dye additives/impurities in commercial dyes affect the microbial activity as well as the biodegradability. The photodegradation (UV/H_2O_2) of non-hydrolyzed Reactive Red 120 in aqueous solutions was studied by Neamtu et al. [24]. Their results showed that 99.6% decoloration was achieved with a dose of 24.5 mmol L^{-1} H_2O_2 at a 60 min irradiation (UV) time (for initial concentration of the dye of 100 mg L^{-1}). Kusvuran et al. [25] tested RR120 degradation using several advanced oxidation processes such as UV/TiO_2, electro-Fenton (EF), wet-air oxidation (WAO) and UV/electro-Fenton (UV/EF). The most efficient method for decoloration and mineralization of RR120 was found to be the WAO process. A novel approach on the RR120 wastewater treatment was proposed by Yakup Arica and Bayramoğlu [42]. During their study, successful biosorption of RR120 dye from aqueous solution by native and modified fungus biomass preparations of Lentinus sajor-caju was reported.

The present study investigates the direct electrooxidation of RR120 in an appropriate supporting electrolyte (1 M $HClO_4$) without further addition of salts or other additives in the azo dye solution using two different types of anodes, Ti/IrO_2–RuO_2 and Si/BDD.

2 Experimental and analytical

2.1 Materials

2.1.1 DSA and BDD preparation

The Ti/IrO_2–RuO_2 electrode was prepared by thermal decomposition of 50 mM H_2IrCl_6 (Acros Organics, 40%) and 50 mM $RuCl_3$ (Fluka 84050, 41%) metal precursors dissolved in isopropanol (Fluka, 99.5%), on a titanium support. The $RuCl_3$ precursor, before the dilution in isopropanol, was stirred and heated at 80 °C for 24 h in a 10% HCl solution. Procedures for the titanium substrate pretreatment and anode deposition are described in previous works [43, 44]. The final IrO_2–RuO_2 loading was 0.5 mg cm^{-2} while the geometrical surface area was 12.5 cm^2.

BDD was prepared by Adamant-Technologies (Switzerland) using the hot filament vapor deposition technique (HF CVD) on single crystal p-type Si wafers. The thickness of the coating was 2 μm, the boron doping was 500 ppm

and the geometrical surface area of the working electrode was 14 cm^2.

2.1.2 Dye solution preparation

Reactive Red 120 ($C_{44}H_{24}Cl_2N_{14}Na_6O_{20}S_6$, shown in Fig. 1) was dissolved in ultra pure water at initial concentrations between 50 and 200 mg L^{-1}. Solutions of 1 M HClO$_4$ were used as supporting electrolyte. Utilization of HClO$_4$ diminishes the generation of extra oxidizing species capable to react with the organic components. In fact, such species could be easily formed if other electrolytes, like NaCl (generation of Cl$_2$), H$_2$SO$_4$ (generation of S$_2$O$_8^{2-}$), FeSO$_4$ (generation of FeO$_4^{2-}$) etc., were used.

2.2 Bulk electrolysis

Electrochemical experiments were conducted in a single-compartment, batch type, laboratory scale electrolytic cell described elsewhere [43, 44]. The volume of the dye solution used in each experiment was 120 mL. All experiments were performed in acidic conditions either at 25 or at 80 °C. The anode was either Ti/IrO$_2$–RuO$_2$ or BDD while two Zr plates were used as cathode. During each electrolytic run, samples of 2 mL were taken from the reactor at certain time intervals and analyzed in terms of COD, TOC and color. A glass tube condenser attached to the reactor was used to prevent evaporation at high temperatures [43, 44].

2.3 Analytical measurements

Chemical oxygen demand (COD) was determined by the dichromate method. The appropriate amount of sample was introduced into a commercially available digestion solution containing potassium dichromate, sulfuric acid and mercuric sulfate (Hach Europe, Belgium) and the mixture was then incubated for 120 min at 150 °C in a COD reactor (Model 45600-Hach Company, USA). COD concentration was measured colorimetrically using a DR/2010 spectrophotometer (Hach Company, USA). Total organic carbon (TOC) was measured by a Shimadzu 5050A TOC analyzer. Changes in sample absorbance were monitored on a Hach-Lange D5000 UV-vis spectrophotometer to assess the

extent of decoloration during treatment. A calibration curve served to correlate the absorbance at 535 nm to RR120 concentration.

Instantaneous current efficiency, ICE, of the anodic oxidation was calculated from changes in COD, as follows:

$$ICE = \frac{\left[(COD)_t - (COD)_{t+\Delta t}\right]}{8I\Delta t}FV \qquad (1)$$

where $(COD)_t$ and $(COD)_{t+\Delta t}$ are the chemical oxygen demand (g O$_2$ m^{-3}) at time t and t+Δt (s) respectively, I is the applied current (A), F is the Faraday constant (C mol^{-1}), V is the volume of the electrolyte (m^3).

3 Results and discussion

3.1 Ti/IrO$_2$–RuO$_2$ anode

Figure 2 shows the effect of the applied current on COD removal at 25 °C as a function of time or applied charge. Higher current densities result in faster COD removal (Fig. 2a) reaching 43% after 5 h at 50 mA cm^{-2}, while the respective value was 32% at 15 mA cm^{-2}. As shown in Fig. 2b, COD removal increases with applied charge but it does not depend on the current density, i.e. applying a fixed charge to achieve a certain COD removal, one may operate either at low currents for long treatment times or vice-versa. Similar behavior was observed at higher temperature, 80 °C (Fig. 3). In this case COD removal reached up to 60% after 26 Ah L^{-1} of charge passed (Fig. 3b). In both temperatures (Figs. 2 and 3) the organic loading decreased within the first 5 h, while further treatment had only a small effect on COD removal.

In order to explore the extent of the oxidation, TOC measurements were performed (Fig. 3). The selective oxidation to organic intermediates appeared to be the main oxidation mechanism especially at 25 °C (Fig. 3a) where the selectivity for partial oxidation products was up to 90% (the maximum TOC removal was only 10%). It is interesting to note that, this value (TOC/TOC$_o$ = 0.9) was achieved in the first few minutes of treatment (2 Ah L^{-1}) and remained constant even after 37 Ah L^{-1} of charge passed. Similar behavior was also observed at higher temperature (80 °C). Although the TOC removal increased

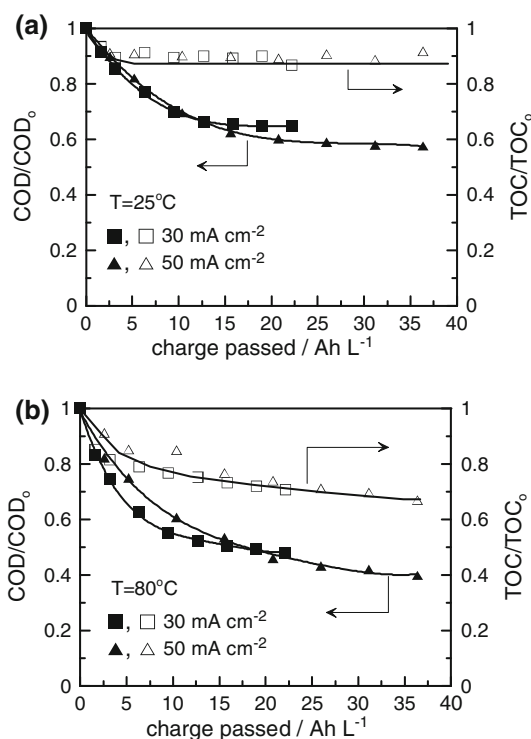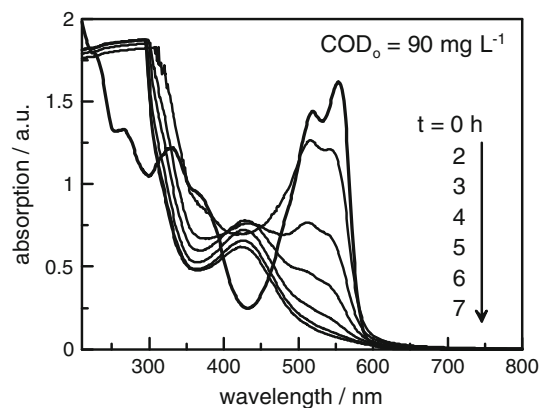**Fig. 1** The structure of Reactive Red 120 (Sigma, CAS 61951-82-4)
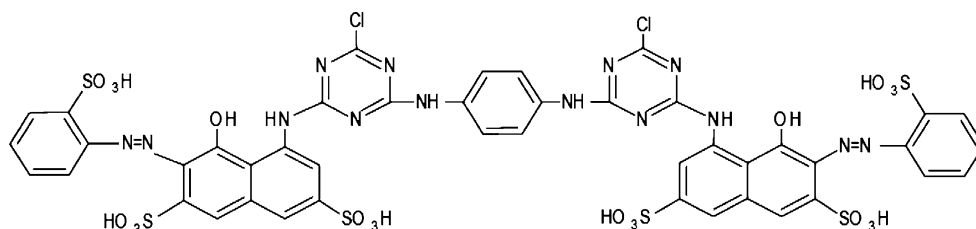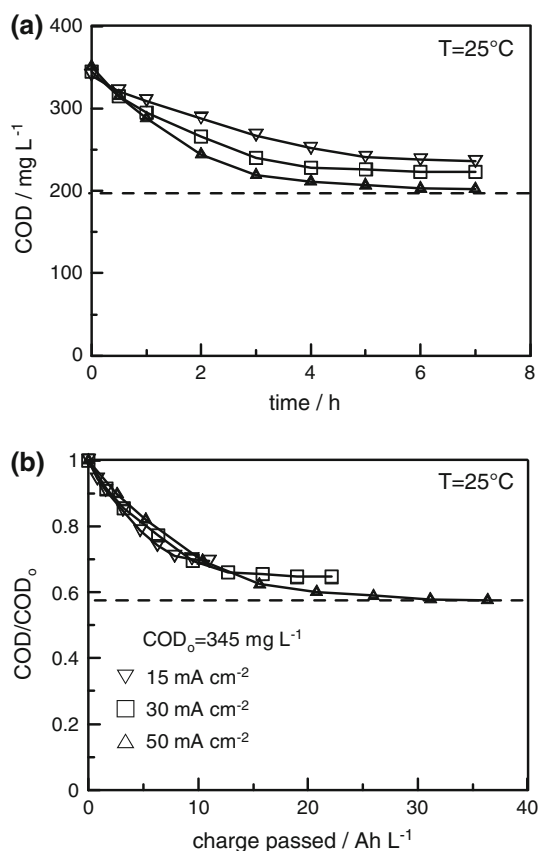
Fig. 2 Effect of applied current density on COD removal as a function of **a** time and **b** charge passed through during electrolysis on Ti/IrO$_2$–RuO$_2$ anode. Conditions: initial concentration of RR120 (C^o_{RR120}) = 0.5 g L^{-1}, i = 15, 30 and 50 mA cm^{-2}, T = 25 °C, 1 M HClO$_4$

Fig. 3 Effect of applied current density on COD and TOC removal as a function of charge passed through during electrolysis on Ti/IrO$_2$–RuO$_2$ anode. Conditions: C^o_{RR120}= 0.5 g L^{-1}, i = 30 and 50 mA cm^{-2}, **a** T = 25 °C and **b** T = 80 °C, 1 M HClO$_4$

up to 32% (at 37 Ah L^{-1}) the partial transformation of RR120 to other organic intermediates was still dominant over the total oxidation to carbon dioxide and water (Fig. 3b).

The presence of transformation by-products was also confirmed by inspection of the UV–visible spectra obtained during electrolysis. Typical spectra for RR120 oxidation (COD$_o$ = 90 mg L^{-1}) at 8 mA cm^{-2} are shown in Fig. 4. The visible band at 535 nm was due to the ring conjugated π system of aromatic rings connected by the azo groups (Fig. 1) [22], while the absorption bands at 265 and 330 nm are attributed to changes in centres with aromatic character. The absorption band at 430 nm (which was not present in the initial spectrum) may be an indication of formation of new organic products. Even after 7 h of treatment, and despite the fact that absorption at 535 nm disappeared, the absorbance at 265 and 330 nm was very high (out of the measurable range) which indicates the existence of aromatic rings. At the same time the absorption at 430 nm was still remarkable indicating the formation of stable reaction intermediates and consequently the

Fig. 4 Evolution of UV–vis spectra with time during electrolysis of Reactive Red 120 on Ti/IrO$_2$–RuO$_2$. Conditions: C^o_{RR120}= 0.15 g L^{-1}, i = 8 mA cm^{-2}, T = 25 °C, 1 M HClO$_4$

preferential behavior of the anode to partial oxidation. Similar spectra have been obtained during all experiments with Ti/IrO$_2$–RuO$_2$ as anode.

Overall, Ti/IrO$_2$–RuO$_2$ behaved like a typical anode with low oxidation power according to the approach proposed by the group of Comninellis [38].
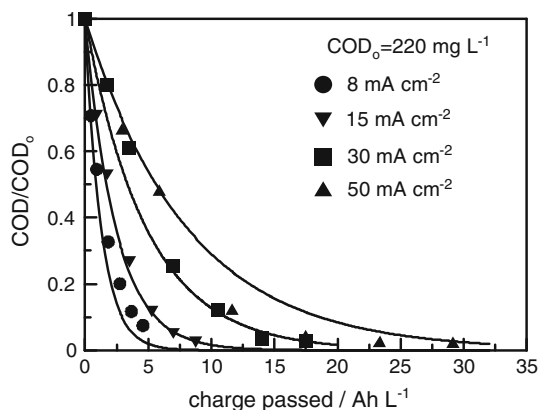
3.2 BDD anode

Figure 5 shows the effect of current density on the electrochemical oxidation of RR120 at 220 mg L^{-1} COD$_o$ as a function of the applied charge at 25 °C. The results showed that COD was almost removed (98%) and this was independent of the conditions studied. Also, there was a remarkable decrease of TOC down to 23% at 8 mA cm^{-2} and down to 90% at 30 mA cm^{-2} (Fig. 6). The curves shown in Fig. 5 are related to the predicted COD changes according to the model developed by Comninellis et al. [45, 46]. This model is capable to predict the temporal evolution of COD and ICE during the electrochemical oxidation of organic pollutants on BDD thin film electrodes. According to this model, if the applied current density (i_{appl}) is greater than the limiting current density (i_{lim}), the electrolysis is mass-transport controlled and secondary reactions (such as oxygen evolution) are involved. In this case, ICE decreases with time while the COD removal, due to mass-transport limitation, follows an exponential trend.

The initial limiting current density ($i_{lim,o}$, A m^{-2}) is related to the initial COD according to the following equation:
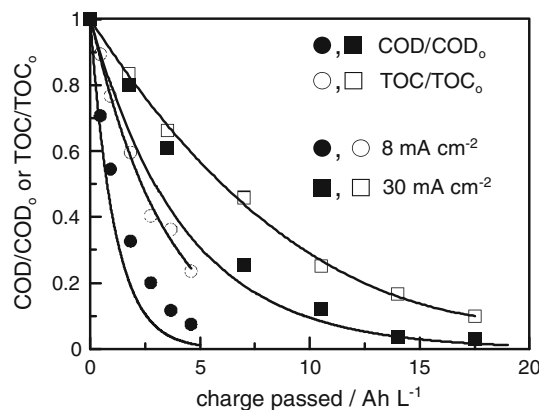
$$i_{lim,o} = 4Fk_mCOD_o \tag{2}$$

where 4 is the number of exchanged electrons, F is Faraday's constant (96,487 C mol^{-1}), k_m is the mass-transport coefficient in the electrochemical reactor (1.72×10^{-5} m s^{-1}) [47] and COD$_o$ is the initial chemical oxygen demand (mol m^{-3}).

In the case where COD$_o$ = 220 mg L^{-1}, application of Eq. 2 yields an initial limiting density of 4.6 mA cm^{-2} (Fig. 5). This means that in all cases the applied current

Fig. 6 Effect of applied current density on COD and TOC removal as a function of charge passed through during electrolysis on BDD anode. The COD curves are the predicted values according to Eq. 3 while TOC curves are fitting lines. Conditions: C^o_{RR120}= 0.33 g L^{-1}, i = 8 and 30 mA cm^{-2}, T = 25 °C, 1 M HClO$_4$
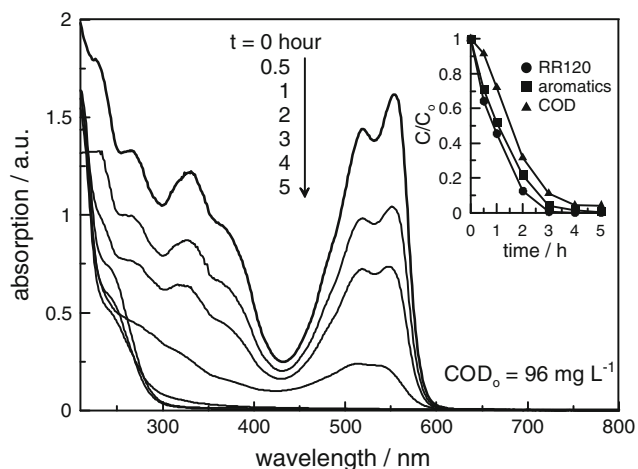
densities (8–50 mA cm^{-2}) were above $i_{lim,o}$. According to the model [45, 46] for $i_{appl} \gg i_{lim}$, COD should change as follows:

$$COD(t) = COD_o \exp\left(-\frac{Ak_m}{V_R}t\right) \tag{3}$$

where A is the electrode area (14×10^{-4} m^2) and V$_R$ is the reactor volume (0.12×10^{-3} m^3).

Based on the results shown in Fig. 5, there is a good agreement between experimental and predicted COD and this is more pronounced at lower current densities.

Figure 7 shows changes in the UV–visible spectra obtained during the electrolysis of RR120 at 96 mg L^{-1} COD$_o$ and 30 mA cm^{-2}. It can been seen that color

Fig. 5 Effect of applied current density on COD removal as a function of charge passed through during electrolysis on BDD anode. Curves show predicted values according to Eq. 3. Conditions: C^o_{RR120}= 0.33 g L^{-1}, i = 8, 15, 30 and 50 mA cm^{-2}, T = 25 °C, 1 M HClO$_4$

Fig. 7 Evolution of UV–vis spectra with time during electrolysis of Reactive Red 120 on BDD. Conditions: C^o_{RR120}= 0.15 g L^{-1}, i = 30 mA cm^{-2}, T = 25 °C, 1 M HClO$_4$. *Inset*: evolution of the normalized concentration of color (λ = 535 nm), aromatics (λ = 330 nm) and COD

removal (measured from changes of absorbance at 535 nm) was faster than the decrease in absorbance at 330 nm and COD, indicating that RR120 oxidation began with breaking the nitro groups (decoloration of the solution) and continued with the cleavage of the aromatic ring (removal of absorbance at 330 and 265 nm) to form aliphatic intermediates, which were finally mineralized to carbon dioxide. Similar behavior has recently been reported for the direct electrochemical oxidation of Acid Yellow 1 [48] and methyl red [33] on BDD.

3.3 Comparison of Ti/IrO$_2$–RuO$_2$ and BDD anodes

Based on the results of this study, Ti/IrO$_2$–RuO$_2$ and BDD showed totally different behavior during the direct anodic electrochemical oxidation of RR120. The rate of the decoloration was much higher in the case of BDD while Ti/IrO$_2$–RuO$_2$, acting as a typical anode with low oxidation power, resulted in partial oxidation products and organic intermediates. Specifically, the formation of new organic compounds was characteristic for Ti/IrO$_2$–RuO$_2$ indicated by the significant absorption band at 430 nm. The cleavage of the aromatic rings was more difficult with Ti/IrO$_2$–RuO$_2$

contrary to the case of BDD where the formation of aliphatic intermediates and their mineralization to carbon dioxide was very fast (Figs. 6, 7).

Another important difference of the two electrodes could be noticed in terms of ICE. The values of ICE obtained with Ti/IrO$_2$–RuO$_2$ were always below 13% (Fig. 8a), while under similar experimental conditions, ICE values up to 45% were observed with BDD (Fig. 8b) at low current density (8 mA cm^{-2}). In both cases, an increase in the current density resulted in a decrease of ICE due to the side reaction of oxygen evolution.

4 Conclusions

Two different types of electrodes have been studied for the direct electrochemical oxidation of Reactive Red 120. Ti/IrO$_2$–RuO$_2$ anode has low oxidation power with high selectivity for organic intermediates and poor TOC removal (10% at 25 °C and 40% at 80 °C), while BDD acting as a typical anode with high oxidation power mineralizes the organic content to CO$_2$. In both cases, the decoloration of the solution was almost 100%. This could be achieved very quickly with BDD (2 Ah L^{-1}) but only after long treatment at high current densities with Ti/IrO$_2$–RuO$_2$ (25 Ah L^{-1}). In the case of the DSA anode and under low current densities, the absorbance in the visible region remained remarkably high even at the end of the treatment. The observed ICE values were always below 0.13 in the case of Ti/IrO$_2$–RuO$_2$, while under the same experimental conditions ICE values up to 0.45 were observed with BDD and low current density (8 mA cm^{-2}).
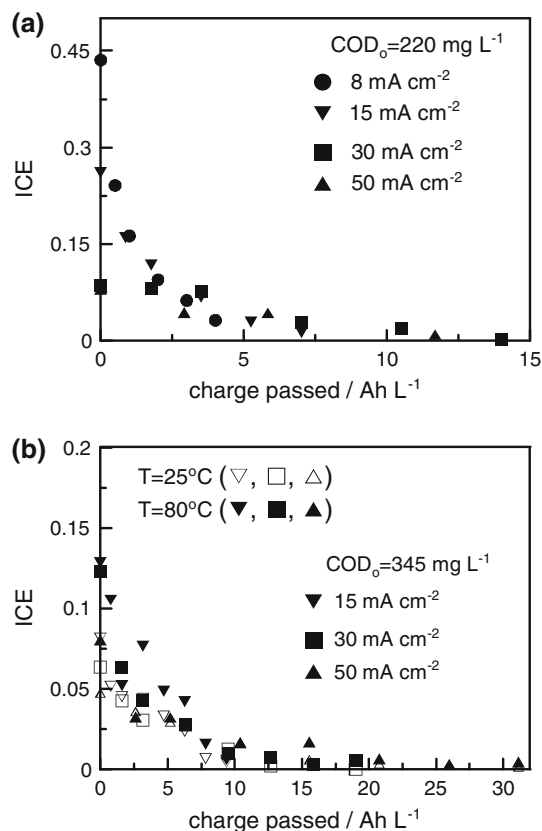
Fig. 8 Variation of ICE during electrolysis of Reactive Red 120 on **a** Ti/IrO$_2$–RuO$_2$ and **b** BDD. Conditions: **a** as in Figs. 2 and 3, **b** as in Fig. 5

References

1. dos Santos AB, Cervantes FJ, van Lier JB (2007) Bioresour Technol 98:2369
2. Christie R (2001) Colour chemistry. The Royal Society of Chemistry, Cambridge
3. Baughman GL, Weber EJ (1994) Environ Sci Technol 28:267
4. Zollinger H (1987) Color chemistry—synthesis, properties and application of organic dyes pigments. VCH, New York
5. Zhou M, He J (2007) Electrochim Acta 53:1902
6. Muthukumar M, Karuppiah MT, Raju GB (2007) Sep Purif Technol 55:198
7. Koparal AS, Yavuz Y, Gurel C, Ogutveren UB (2007) J Hazard Mater 145:100
8. Rajkumar D, Song BJ, Kim JG (2007) Dyes Pigments 72:1
9. Oliveira FH, Osugi ME, Paschoal FMM, Profeti D, Olivi P, Zanoni MVB (2007) J Appl Electrochem 37:583
10. Rajkumar D, Kim JG (2006) J Hazard Mater 136:203

11. Vaghela SS, Jethva AD, Mehta BB, Dave SP, Adimurthy S, Ramachandraiah G (2005) Environ Sci Technol 39:2848
12. Sanroman MA, Pazos M, Cameselle C (2004) J Chem Technol Biotechnol 79:1349
13. Sakalis A, Vanarkova D, Holaapek M, Jandera P, Voulgaropoulos A (2007) Chemosphere 67:1940
14. Xiong Y, Strunk PJ, Xia H, Zhu X, Karisson HT (2001) Water Res 35:4226
15. Fan L, Zhou Y, Yang W, Chen G, Yang F (2006) J Hazard Mater 137:1182
16. Carneiro PA, Osugi ME, Fugivara CS, Boralle N, Furlan M, Zanoni MVB (2005) Chemosphere 59:431
17. Cameselle C, Pazos M, Sanromán MA (2005) Chemosphere 60:1080
18. Lopes A, Martins S, Morao A, Magrinho M, Goncalves I (2004) Electrochim Acta 22:279
19. Pacheco MJ, Ciriaco MLF, Lopes A, Concalves IC, Nunes MR, Pereira MI (2006) Port Electrochim Acta 24:273
20. Canizares P, Gadri A, Lobato J, Nasr B, Paz R, Rodrigo MA, Saez C (2006) Ind Eng Chem Res 45:3468
21. Chen X, Chen G, Yue PL (2003) Chem Eng Sci 58:995
22. Zhang F, Yediler A, Liang X (2007) Chemosphere 67:712
23. Zhang F, Yediler A, Liang X, Kettrup A (2004) Dyes Pigments 60:1
24. Neamtu M, Siminiceanu I, Yediler A, Kettrup A (2002) Dyes Pigments 53:93
25. Kusvuran E, Gulnaz O, Irmak S, Atanur OM, Yavuz HI, Erbatur O (2004) J Hazard Mater 109:85
26. Martinez-Huitle CA, Brillas E (2009) Appl Catal B: Environ 87:105
27. Villanueva-Rodriguez M, Hernandez-Ramirez A, Peralta-Hernandez JM, Bandala ER, Quiroz-Alfaro MA (2009) J Hazard Mater 167:1226
28. Daneshvar N, Khataee AR, Amani Ghadim AR, Rasoulifard MH (2007) J Hazard Mater 148:566
29. Parsa JB, Rezaei M, Soleymani AR (2009) J Hazard Mater 168:997
30. Alinsafi A, Khemis M, Pons MN, Leclerc JP, Yaacoubi A, Benhammou A, Nejmeddine A (2005) Chem Eng Proc: Proc Intens 44:461
31. Catanho M, Malpass GRP, Motheo AJ (2006) Appl Catal B: Environ 62:193
32. del Rio AI, Molina J, Bonastre J, Cases F (2009) Chemosphere 75:1329
33. Panizza M, Cerisola G (2008) Ind Eng Chem Res 47:6816
34. Panizza M, Cerisola G (2007) Appl Catal B: Environ 75:95
35. Sakalis A, Fytianos K, Nickel U, Voulgaropoulos A (2006) Chem Eng J 119:127
36. Chatzisymeon E, Xekoukoulotakis NP, Coz A, Kalogerakis N, Mantzavinos D (2006) J Hazard Mater 137:998
37. Kusvuran E, Irmak S, Yavuz HI, Samil A, Erbatur O (2005) J Hazard Mater 119:109
38. Kapałka A, Foti G, Comninellis C (2008) J Appl Electrochem 38:7
39. Comninellis C (1994) Electrochim Acta 39:1857
40. Martinez-Huite CA, Ferro S (2006) Chem Soc Rev 35:1324
41. Panizza M, Cerisola G (2005) Electrochim Acta 51:191
42. Arica MY, Bayramoglu G (2007) J Hazard Mater 149:499
43. Chatzisymeon E, Dimou A, Mantzavinos D, Katsaounis A (2009) J Hazard Mater 167:268
44. Papastefanakis N, Mantzavinos D, Katsaounis A (2010) J Appl Electrochem 40:729
45. Panizza M, Michaud PA, Cerisola G, Comninellis C (2001) J Electroanal Chem 507:206
46. Panizza M, Michaud PA, Cerisola G, Comninellis C (2001) Electrochem Commun 3:336
47. Chatzisymeon E, Xekoukoulotakis NP, Diamadopoulos E, Katsaounis A, Mantzavinos D (2009) Water Res 43:3999
48. Rodriguez J, Rodrigo MA, Panizza M, Cerisola G (2009) J Appl Electrochem 39:2285